Bone morphogenetic protein 4 in the extraembryonic mesoderm is required for allantois development and the localization and survival of primordial germ cells in the mouse

Takeshi Fujiwara*, N. Ray Dunn*†, and Brigid L. M. Hogan*‡§

*Department of Cell Biology, Vanderbilt University Medical Center, and ‡Howard Hughes Medical Institute, 1161 21st Avenue South, Nashville, TN 37232-2175

Communicated by R. L. Brinster, University of Pennsylvania, Philadelphia, PA, September 26, 2001 (received for review July 3, 2001)

Evidence suggests that the specification of primordial germ cells (PGCs) in the mammalian embryo does not depend on maternal determinants. Rather, previous genetic analysis in the mouse has shown that bone morphogenetic protein 4 (Bmp4) is required for the formation of both PGCs and allantois. Bmp4 is expressed in both the trophoblast-derived extraembryonic ectoderm (ExE) and in the epiblast-derived extraembryonic mesoderm (ExM), in which the PGCs, allantois primordium, and angioblasts are first detected. We have shown that Bmp4 made in the ExE functions to induce precursors of PGCs and allantois in the adjacent epiblast, resulting in complete lack of both cell types in homozygous null mutants. However, the function of Bmp4 in the ExM is totally unknown. To address this question, we generated tetraploid (4N) chimeras by aggregating *Bmp4* null ES cells with wild-type tetraploid embryos. In this combination, wild-type tetraploid cells contribute to the extraembryonic trophoblast and primitive endoderm lineages but are excluded from the epiblast and its derivatives, including the ExM. Our results clearly demonstrate that Bmp4 made in the ExM does not affect the establishment of either PGC or allantois lineages, but is required for PGC localization and survival and for the differentiation of the allantois. These findings suggest that *Bmp4* expressed in epiblast-derived tissues plays vital roles in reproduction by regulating both the development of the germ line and the vascular connection between the embryo and the placenta.

In the mouse embryo, primordial germ cells (PGCs) are first detected at the head-fold stage as a cluster of about 45 alkaline phosphatase (AP)-expressing cells at the base of the allantois (1). These PGCs subsequently migrate into the endoderm that gives rise to the hindgut (2), distribute along the hindgut, and finally move through the dorsal mesentery into the genital ridges (reviewed in ref. 3). Lineage analysis has shown that the PGCs are derived before gastrulation from a subpopulation of proximal epiblast cells adjacent to the trophoblast-derived extraembryonic ectoderm (ExE). Significantly, these precursors are not lineage restricted but have descendants in both the germ line and extraembryonic tissues, such as the allantois, yolk sac mesoderm, and amnion (1).

Previous studies suggest that the specification of the mouse germ line does not involve, as in many other organisms, the inheritance of maternal determinants. Rather, it appears that interactions between the trophoblast-derived ExE and the adjacent epiblast first establish precursors that can give rise to both PGCs and extraembryonic mesoderm cells. A second process then allocates descendants of these cells to the different lineages (reviewed in ref. 3). This model says nothing about whether the interactions induce the *de novo* expression of genes specifically required for PGC development, or whether they maintain in the PGCs expression of key factors permitting pluripotency that are normally lost in cells that differentiate into somatic lineages. Moreover, the induction of the PGC/allantois precursors may be a cumulative process, initiated by signaling between the trophoblast and the inner cell mass (ICM) of the blastocyst and continued between the ExE and the proximal epiblast.

The idea that interactions between the ExE and epiblast are required for PGC development is supported by experimental and genetic evidence. For example, if epiblast cells of the prestreak embryo are cultured in contact with the ExE, some of the epiblast cells differentiate into AP-positive, presumptive PGCs (4). Moreover, studies suggest that this interaction is mediated by extracellular signaling proteins, including bone morphogenetic proteins (Bmps) Bmp4 and Bmp8b, both of which are expressed in the ExE. Thus, *Bmp4* homozygous null mutants completely lack PGCs and an allantois, whereas *Bmp8b* homozygous null mutants have either a significantly reduced number of PGCs or none at all, and poor development of the allantois (5–7). Culture of distal epiblasts with cells expressing Bmp4 and Bmp8b results in the appearance of AP-positive, presumptive PGCs after about 72 h (8).

In addition to its expression in the ExE, *Bmp4* is also transcribed in the extraembryonic mesoderm (ExM). At the late streak stage, *Bmp4*-expressing cells are predominantly localized at the periphery of the incipient allantois bud, abutting the exocoelom and separated from the cluster of PGCs by a population of non-*Bmp4*-expressing mesenchyme cells. By the head-fold stage, *Bmp4*-expressing cells are more extensively distributed within the allantois, and some are seen adjacent to the PGCs (ref. 5 and Fig. 4 *B* and *C*). Taken together, these results suggest that Bmp4 has the potential to affect PGC and allantois development at several different steps: first, in a dose-dependent way in the establishment of precursors in the epiblast, then in the allocation of these precursors to the PGC or allantois lineages, and finally in the survival and differentiation of these cell types once they have been specified.

In this paper, we test the last two hypotheses by performing tetraploid chimera analysis. Lines of $Bmp4^{lacZ/tm1}$ null embryonic stem (ES) cells were established and aggregated with wild-type tetraploid (4N) morulae to generate chimeric embryos (9). With this strategy, the trophoblast and ExE will express *Bmp4* (and *Bmp8b*), and the primitive endoderm-derived visceral endoderm

DEVELOPMENTAL BIOLOGY

Abbreviations: Bmp, bone morphogenetic protein; PGC, primordial germ cell; ExE, extraembryonic ectoderm; ExM, extraembryonic mesoderm; ES, embryonic stem; 4N, tetraploid; AP, alkaline phosphatase; ICM, inner cell mass; VCAM-1, vascular cell adhesion molecule 1.

†Present address: Department of Molecular and Cellular Biology, Harvard University, Cambridge, MA 02138.

§To whom reprint requests should be addressed at: Department of Cell Biology, Vanderbilt University Medical Center, C-2310 MCN, Nashville, TN 37232-2175. E-mail: brigid.hogan@mcmail.vanderbilt.edu.

The publication costs of this article were defrayed in part by page charge payment. This article must therefore be hereby marked "*advertisement*" in accordance with 18 U.S.C. §1734 solely to indicate this fact.

will express *Bmp2* (7), but the ICM derivatives, including the ExM, will completely lack *Bmp4* expression. We find that these chimeric embryos do contain PGCs at the presomite stage, in about the same number as control chimeras. However, most of the PGCs are incorrectly localized in the yolk sac, from which they later disappear. Mutant tetraploid chimeras also show abnormal development of the allantois, which fails to extend and fuse with the chorion and lacks a normal vasculature. We conclude that Bmp4 expressed in the ExM is not required for the allocation of precursors into the PGC and allantois/ExM lineages but does affect the subsequent behavior and survival of the PGCs and the differentiation of the allantois.

Materials and Methods

Excision of the Floxed neo^r Cassette in *Bmp4^{lacZneo}* ES Cells and Generation of Transheterozygous Bmp4 Null ES Cells. 12C *Bmp4^{lacZneo}* ES cells (50×10^6) (5) were electroporated with 100 μg of cytomegalovirus (pCMV)-*Cre* plasmid. The *neo* excised clones were screened by Southern blot analysis of *Spe*I-digested genomic DNA with the 5′ external 500-bp *Bsm*I–*Bam*HI *Bmp4* genomic probe (10). One clone, 10G, was chosen for the generation of transheterozygous *Bmp4* null ES cell lines. 10G ES cells (16.4×10^6) were electroporated with 50 μg of *Not*I-linearized V_b replacement vector, which targets exons 1 and 2 of the *Bmp4* allele with a *neo* (neomycin-resistance) gene (10). Clones were screened by Southern blot analysis of *Xba*I-digested genomic DNA with the 5′ external *Bmp4* genomic probe as described. Five of 142 clones were identified as *Bmp4$^{lacZ/tm1}$* transheterozygous null lines (data not shown). Two lines, 5H and 6H, were chosen for further investigation by chimeric analysis. The heterozygous *Bmp4$^{lacZ/+}$* line, 3E, was used as a control.

Generation of Tetraploid Chimeric Embryos. Tetraploid embryos were produced by aggregating four-cell stage tetraploid embryos with 12–16 ES cells as described (9).

β-Galactosidase Staining and Detection of PGCs. β-Galactosidase staining, histological analysis, and whole-mount AP staining of tetraploid chimeric embryos were performed as described (5).

Whole-Mount Immunostaining. Whole-mount immunostaining was performed as described (11). Embryos were exposed to primary antibodies against Pecam1 (PharMingen), Flk1 (PharMingen), or vascular cell adhesion molecule 1 (VCAM-1) (PharMingen) at a dilution of 1:150. Horseradish peroxidase-conjugated donkey anti-rat IgG (Jackson ImmunoResearch) was used as a secondary antibody at a dilution of 1:1,000. Antibody binding was detected with the use of diaminobenzidine hydrochloride substrate.

Cell Proliferation Assay. Embryos were fixed and stained for β-galactosidase activity as described above. After fixation in 4% paraformaldehyde/PBS for 1 h at 4°C embryos were dehydrated in 100% isopropyl alcohol, embedded in wax, and serially sectioned at 7 μm. Anti-phosphohistone H3 antibody staining of serial sections was performed after antigen retrieval in 10 mM sodium citrate solution. Sections were exposed to the primary antibody at 1:500 dilution in normal donkey serum overnight at room temperature. After three 15-min changes of PBS they were exposed to secondary Cy3-conjugated donkey anti-rabbit IgG (Jackson ImmunoResearch) at 1:1,000 dilution for 1 h at 4°C. After three 15-min changes of PBS, YO-PRO-1 (Molecular Probes) was used at 1:5,000 dilution in PBS for nuclear counterstaining. Slides were mounted with 50% glycerol/2% *n*-propyl gallate/PBS, and the number of positive and negative nuclei in all sections was counted.

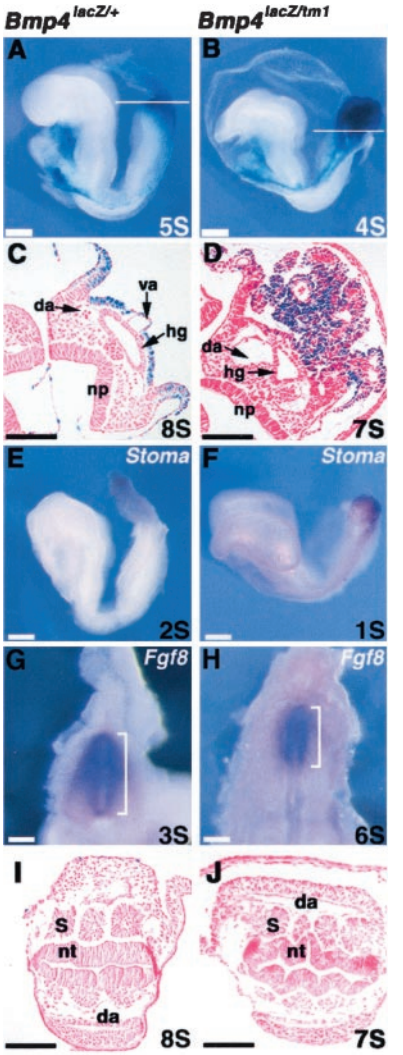

Fig. 1. Morphology and posterior differentiation of tetraploid chimeras. (*Left*) *Bmp4$^{lacZ/+}$* chimeras. (*Right*) *Bmp4$^{lacZ/tm1}$* chimeras. (*A* and *B*) Lateral views of five-somite (5S; *A*) and four-somite (4S; *B*) tetraploid chimeras after staining with 5-bromo-4-chloro-3-indolyl β-D-galactoside (X-Gal) to reveal *Bmp4^{lacZ}* expression. Both chimeras show expression in the allantois, amnion, lateral plate mesoderm, and heart. Note the well-formed, extended allantois in the control (*A*) and unextended allantois in the null mutant chimera (*B*). (*C* and *D*) Section through posterior of seven- or eight-somite chimeras in a plane similar to that indicated in *A* and *B*. Embryos were stained with X-Gal, and sections were counterstained with eosin. Note the close proximity of the mutant allantois to the posterior of the embryo and the presence of some blood vessels within the tissue (*D*). No vitelline artery can be seen in this or adjacent sections of the mutant chimera. (*E* and *F*) Whole-mount *in situ* hybridization of one- or two-somite stage chimeras with *Stoma* probe. (*G* and *H*) Reduced posterior primitive streak in mutant tetraploid chimera. Posterior view of two chimeras after whole-mount *in situ* hybridization with *Fgf8* probe. Note that the null mutant chimera is at the six-somite stage, whereas the control chimera is at the three-somite stage. (*I* and *J*) Section through the same chimera as in *C* and *D*. Note the abnormal morphology of the neural tube and somites in the mutant (*J*). da, Dorsal aorta; hg, hindgut; np, neural plate; nt, neural tube; s, somite; va, vitelline artery. (Scale bars: *A*, *B*, *E*, and *F*, 200 μm; *C*, *D*, *G*–*J*, 100 μm.)

Results

Generation of Tetraploid Chimeras with *Bmp4$^{lacZ/tm1}$* Null ES Cell Lines. Tetraploid chimeras were generated by aggregating *Bmp4$^{lacZ/tm1}$* null ES cells (see *Materials and Methods*) with wild-type 4N ICR embryos. At the early somite stage, *Bmp4$^{lacZ/tm1}$* ↔ wild-type

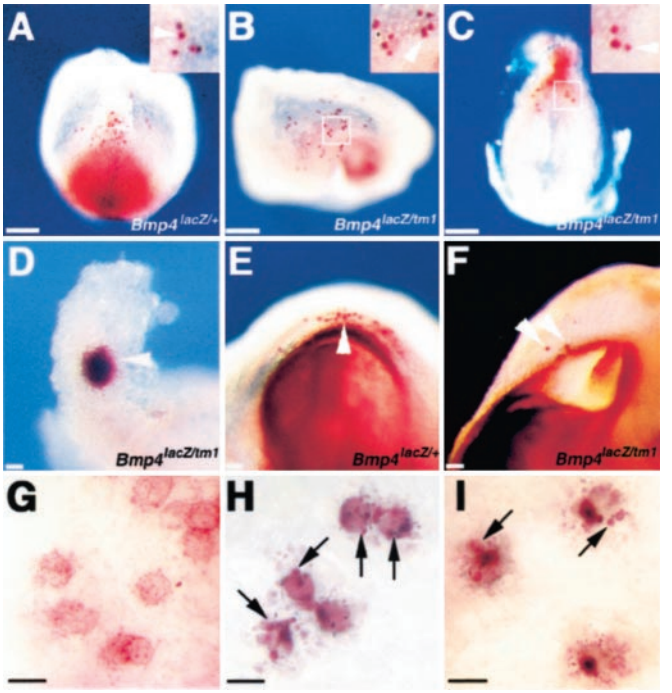

Fig. 2. PGCs in tetraploid chimeras. Whole-mount AP staining of $Bmp4^{lacZ/+}$ (*A* and *E*) and $Bmp4^{lacZ/tm1}$ (*B–D* and *F*) chimeras. PGCs are indicated by arrowheads. At the presomite stage in the control chimera (*A*) most PGCs are detected at or near the base of the allantois. One mutant chimera gave a similar distribution (not shown). In two mutant chimeras, PGCs were more dispersed within the yolk sac, as shown in the posterior–lateral view in *B*. In a fourth chimera (*C* and *D*) PGCs were seen in both the posterior endoderm (*C*) and a large clump of AP-positive cells in the allantois (*D*). At the four-somite stage, PGCs are detected in the forming hindgut pocket of control chimeras (*E*), but only very few are seen in mutant chimeras (*F*). *Insets* in *A*—*C* are higher magnifications of the boxed areas. (*G–I*) Morphology of AP-stained PGCs in *A–C*. In the control chimera, PGCs at the base of the allantois had a regular rounded morphology (*G*). In mutant chimeras, most PGCs within the yolk sac (*H*) and at the base of allantois (*I*) showed numerous large cytoplasmic blebs (arrows). (Scale bars: *A*—*C*, 200 μm; *D–I*, 100 μm.)

tetraploid chimeras (hereafter referred to as $Bmp4^{lacZ/tm1}$ tetraploid chimeras) were somewhat smaller than control chimeras (Fig. 1 *A* and *B*). In wild-type embryos and $Bmp4^{lacZ/+}$ tetraploid chimeras at this stage, the allantois has grown toward the chorion and has started to fuse with it. However, in 14 of the 16 $Bmp4^{lacZ/tm1}$ tetraploid chimeras analyzed here, the allantois was small and unextended and remained closely associated with the posterior of the embryo (Fig. 1 *A–D*). In the other two chimeras, the allantois was ballooned out but had not fused with the chorion (Fig. 3*C*, *c* and *d*).

To determine whether the allantoic mesoderm had been specified correctly, we attempted to determine whether the cells express *Stoma*. This gene normally has a very restricted expression pattern and is transcribed strongly in the early allantois (A. Shimono and R. Behringer, personal communication). Strong localized expression of *Stoma* was observed in both $Bmp4^{lacZ/+}$ and $Bmp4^{lacZ/tm1}$ tetraploid chimeras, suggesting that mesoderm cells can be specified as allantois in the absence of *Bmp4* expression in the ExM (Fig. 1 *E* and *F*). Moreover, expression of *Fgf8* was used to assess primitive streak formation (12). Whole-mount *in situ* hybridization analysis revealed that in the $Bmp4^{lacZ/tm1}$ tetraploid chimeras the primitive streak was indeed formed but was somewhat shorter than normal (Fig. 1 *G* and *H*). Finally, histological analysis of the mutant chimeras showed complete lack of the vitelline artery as well as aberrant development of the neural tube and somites (Fig. 1 *I* and *J*).

PGC Development in $Bmp4^{lacZ/tm1}$ Tetraploid Chimeras. To test the role of Bmp4 made in the ExM on PGC development, chimeric embryos were subjected to whole-mount AP staining. At the presomite stage most of the PGCs in the four control $Bmp4^{lacZ/+}$ tetraploid chimeras analyzed were detected in their normal location at the base of allantois. A few were seen in the yolk sac, but none were seen within the allantois (Fig. 2*A* and Table 1). At high magnification after AP staining, wild-type PGCs had a regular, rounded appearance (Fig. 2*G*). In contrast, in $Bmp4^{lacZ/tm1}$ tetraploid chimeras at this stage most PGCs were found dispersed in ectopic sites (yolk sac, amnion, and allantois), with fewer at the base of the allantois (Fig. 2 *B* and *C* and Table 1). In one of the four mutant chimeras analyzed there was a large clump of presumptive PGCs inside the allantois (Fig. 2*D*), so it was not possible to ascertain the total number of PGCs in this chimera. Significantly, the overall number of countable PGCs did not differ between the two classes of chimeras. In the $Bmp4^{lacZ/+}$ tetraploid chimeras there were 37 ± 6 PGCs (n = 4), whereas in the $Bmp4^{lacZ/tm1}$ tetraploid chimeras there were 40 ± 5 PGCs (n = 3). At high magnification, most PGCs, both at the base of the allantois and in the yolk sac, had an irregular appearance and numerous large cytoplasmic "blebs," as might be expected if the cells were not adhering to the substratum or were about to undergo apoptosis (Fig. 2 *H* and *I*).

At the two- to five-somite stage, a dramatic difference was seen between the two kinds of chimera in terms of PGC number. In the four $Bmp4^{lacZ/+}$ tetraploid chimeras analyzed at this stage most PGCs (38 ± 5) were closely associated with the hindgut pocket. However, in the $Bmp4^{lacZ/tm1}$ tetraploid chimeras, only 12 ± 8 PGCs (n = 4) were observed in this location (Fig. 2 *E* and *F* and Table 1). The number of PGCs in the yolk sac was significantly reduced to 3 ± 3 from 21 ± 10 in the presomite stage (Table 1). In the one $Bmp4^{lacZ/tm1}$ tetraploid chimera analyzed at the seven-somite stage, no detectable PGCs were observed (Table 1). Taken together, our findings suggest that Bmp4 produced in the ExM is required for the proper localization and survival of PGCs once they are specified.

Abnormal Development of the Allantois in Mutant Chimeras. In the normal embryo several processes contribute to the growth,

Table 1. Number of PGCs in respective somatic cells

Stage	Genotype	No. of PGCs in region					
		Base of allantois	Hindgut	Yolk sac	Allantois	Amnion	Overall
Presomite	$Bmp4^{lacZ/+}$ (4)	32 ± 4		5 ± 3	1 ± 1	1 ± 1	37 ± 6
	$Bmp4^{lacZ/tm1}$ (3)	14 ± 7		21 ± 10	2 ± 2 (2)	2 ± 2	40 ± 5
Two to five somites	$Bmp4^{lacZ/+}$ (4)		38 ± 5	0	4 ± 2	0	42 ± 5
	$Bmp4^{lacZ/tm1}$ (4)		12 ± 8	3 ± 3	8 ± 7	1 ± 1	20 ± 8
Seven somites	$Bmp4^{lacZ/tm1}$ (1)		0	0	2	0	2

Results are presented as mean ± SD. Numbers in parentheses are number of chimeric embryos examined.

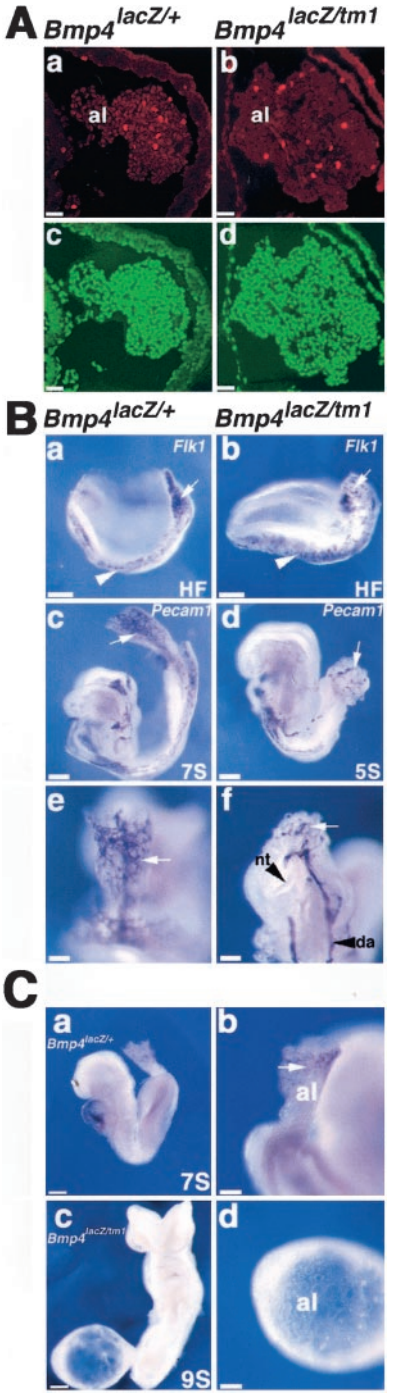

Fig. 3. Proliferation, vascularization, and mesothelium formation in the allantois in tetraploid chimeras. (*A*) Cell proliferation in the allantois. Sections are through the posterior of four-somite-stage chimeras, in a plane similar to that indicated in Fig. 1 *A* and *B*. (*Left*) *Bmp4*$^{lacZ/+}$ chimeras. (*Right*) *Bmp4*$^{lacZ/tm1}$ chimeras. (*a* and *b*) Immunofluorescence staining with antibody to phosphohistone H3. (*c* and *d*) Counterstaining with Yo-Pro-1 to reveal all nuclei. (*B*) Vascularization of the allantois. (*Left*) *Bmp4*$^{lacZ/+}$ chimeras. (*Right*) *Bmp4*$^{lacZ/tm1}$ chimeras. (*a* and *b*) Whole-mount immunostaining of headfold (HF)-stage chimeras with antibody to Flk1. Note the lower number of positive cells (arrows) in the allantois of the mutant tetraploid chimera (*b*) compared with control (*a*). No significant difference was seen in the lateral plate (arrowheads). (*c–f*) Whole-mount immunostaining of seven-somite- (*c* and *e*) and five-somite- (*d* and *f*) stage chimeras with antibody to Pecam1. The allantois of the control chimera (*c*) shows a complex network of blood vessels (arrow), illustrated at higher power magnification in *e*. In contrast, the mutant allantois (*d* and *f*) has few vessels (arrows). Note the kinked neural tube (arrowhead) in *f*. (*C*) Differentiation of the mesothelium: (*Upper*) *Bmp4*$^{lacZ/+}$ chimera at seven-somite stage and (*Bottom*) *Bmp4*$^{lacZ/tm1}$ chimera at nine-somite stage, both after whole-mount immunostaining with antibody to VCAM-1. (*b*) Higher magnification of chimera in *a*, showing VCAM-1 expression (arrows) in the distal cells of the allantois. (*d*) Higher magnification of the chimera in *c*, showing the absence of VCAM-1 expression in the distal cells of the balloon-like allantois. al, Allantois; da, dorsal aorta; nt, neural tube. [Scale bars: *A* (*a–d*), *B* (*e* and *f*), and *C* (*b* and *d*), 100 μm; *B* (*a–d*) and *C* (*a* and *c*), 200 μm.]

elongation, and differentiation of the allantois once the primordium of this tissue has been established (13–15). Initially, the allantois increases in size because of the recruitment of cells from the posterior primitive streak. By the two- to three-somite stage, cell proliferation and cavitation take over as the most important driving forces of expansion. At the same time, there is distal–proximal differentiation of Flk1-expressing angioblasts within the allantois and organization of endothelial cells into a network of Pecam1-positive blood vessels. Significantly, these latter events occur by local vasculogenesis, and not by invasion of the vitelline or fetal blood vessels from the embryo, and there is no accompanying erythropoiesis. Finally, first the distal, and then more proximal, cells of the allantois differentiate into a mesothelium expressing the gene encoding VCAM-1.

To determine whether the morphological defect of the allantois of the mutant chimeras is due to reduced proliferation, we carried out immunohistochemistry with the use of anti-phosphohistone H3 antibody, which detects cells in G_2 and mitosis. The ratio of phosphohistone H3-positive cells within the entire allantoic mesoderm was 5.0% $\pm$ 0.7% in the *Bmp4*$^{lacZ/tm1}$ tetraploid chimera compared with 4.6% $\pm$ 0.7% in the control (Fig. 3*A*, *a–d*), suggesting that there was no significant difference in the proliferation rates of the two tissues.

To examine vascularization in the mutant chimeras, we performed whole-mount immunohistochemistry with antibodies to Flk1 and Pecam1. Within the yolk sac and lateral plate mesoderm of both *Bmp4*$^{lacZ/tm1}$ and *Bmp4*$^{lacZ/+}$ tetraploid chimeras, there was little difference in the level of Flk1-positive cells (Fig. 3*B*, *a* and *b*, and data not shown), indicating that mesoderm can differentiate into angioblasts, despite the lack of *Bmp4* expression in the ExM. In contrast, in the allantois of the *Bmp4*$^{lacZ/tm1}$ tetraploid chimeras, the level of Flk1-positive cells was reduced compared with controls (Fig. 3*B*, *a* and *b*). Moreover, the number and complexity of blood vessels were also dramatically reduced in the allantois region, as revealed by Pecam1 staining (Fig. 3*B*, *c–f*).

Two of the 16 *Bmp4*$^{lacZ/tm1}$ tetraploid chimeras analyzed had an abnormal balloon-shaped allantois that failed to fuse with the chorion (Fig. 3*C*, *c* and *d*). This phenotype resembled that of embryos homozygous null for either VCAM-1 or α4 integrin, genes that encode surface molecules mediating specific adhesion between expressing cells (16–18). In mouse embryos from embryonic day 7.5 to 9.5, VCAM-1 is normally expressed in the distal mesothelial cells of the allantois that mediate chorioallantoic fusion by interacting with α4 integrin-expressing cells in the chorion and in some internal mesenchyme cells (19). Whole-mount immunohistochemistry with an anti-VCAM-1 antibody revealed protein at the distal end of the allantois in the *Bmp4*$^{lacZ/+}$ tetraploid chimera (Fig. 3*C*, *a* and *b*). However, staining was not seen in *Bmp4*$^{lacZ/tm1}$ chimera (Fig. 3*C*, *c* and *d*), suggesting that Bmp4 signaling is required for VCAM-1 expression in the developing allantois.

Discussion

Role of Bmp4 in Establishing the Germ Cell Lineage. Previous analysis of *Bmp4* null mutant embryos showed that they completely lack both PGCs and an allantois, whereas *Bmp8b* null embryos have few or no PGCs and a small allantois (5–8). Because *Bmp4* and

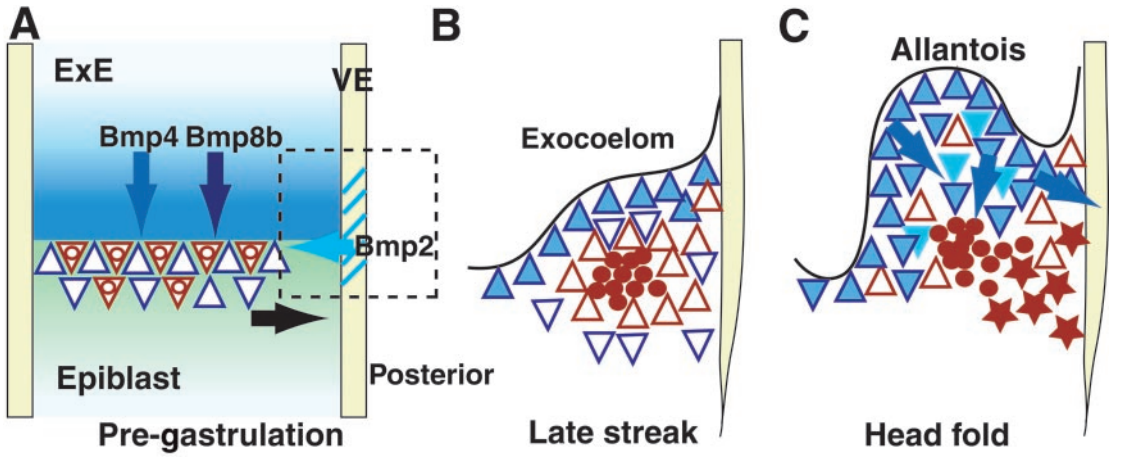

Fig. 4. Model for the role of Bmp signaling in early PGC development in the mouse. (*A*) Before gastrulation. Bmp4 and Bmp8b, produced together in the extraembryonic ectoderm (ExE), and Bmp2 in the visceral endoderm (VE) function together to induce precursors of PGCs and extraembryonic mesoderm (ExM) in the proximal epiblast. At this stage epiblast cells are not lineage restricted, and single cells, denoted here by red triangles with inner circles, can give rise to descendants in the PGCs, allantois, and ExM. Other cells (blue triangles) give rise to descendants in the allantois and ExM, but not PGCs. Evidence suggests that Bmp4 and Bmp8b act on the epiblast cells through different receptors (8), and Smad5 also plays a role at this stage (25). (*B*) Late streak-incipient allantois bud stage: high magnification of the posterior region boxed in *A*, excluding the primitive streak. By this stage the allocation of cells to the PGC (red circles) and somatic cell (red triangle) lineages has taken place. Bmp4 expression is seen in mesoderm cells adjacent to the exocoelom but not immediately around the PGCs (5). (*C*) Headfold stage. Somatic cells within the allantois express Bmp4 (dark blue) and Bmp2 (light blue). PGCs are no longer in a tight clump and move (red stars) to the endoderm of the future hindgut (2). Bmp4 may affect PGC migration and survival directly, or indirectly by affecting the differentiation of the ExM and/or the endoderm (blue arrows). In the absence of *Bmp4* or *Smad5* (25), PGCs may be swept passively into ectopic locations by expansion of the allantois and yolk sac or may no longer be prevented from moving there.

Bmp8b are coexpressed in the ExE before gastrulation it was proposed that the two signaling proteins function in a dose-dependent manner to establish PGC/allantois precursors in the proximal epiblast. This hypothesis was supported by the finding that wild-type ES cells are unable to rescue the PGC and allantois phenotype when combined with $Bmp4^{tm1}$ $-/-$ embryos, either by blastocyst injection or by morula aggregation (5).

The reciprocal tetraploid chimera experiments described here are also consistent with the hypothesis that the formation of PGC precursors in the proximal epiblast absolutely requires Bmp4 made by the trophoblast/ExE and does not, as suggested by others (8), depend upon any Bmp4 expression in ICM cells at the blastocyst stage (20). This interpretation assumes that in the chimeras the host wild-type 4N embryos never contribute any cells to the ICM of the blastocyst. However, it could be argued that a few 4N cells are present transiently in the ICM before being competed out by 2N cells, and that they produce enough Bmp4 protein to maintain a subpopulation of ICM cells containing cell autonomous factors permissive for the pluripotent state. However, we consider this possibility unlikely, for two reasons. First, genetic evidence suggests that Bmp4 functions in a dose-dependent way in establishing PGCs. Because the number of transient 4N cells in the ICM would likely be small, the alternative model would predict significantly fewer founder PGCs in mutant chimeras than in controls, which was not observed. Second, our previous chimera experiments showed that a high proportion of wild-type ES cells, which presumably would make Bmp4 in the ICM, failed to rescue PGC formation in *Bmp4* $-/-$ embryos (5).

The fact that both founder PGCs and allantois cells are present in $Bmp4^{lacZ/tm1}$ tetraploid chimeras rules out the possibility that Bmp4 plays a role in the allocation of common precursor cells to either germ-line or somatic lineages. Other factors as yet unknown are therefore likely to control this decision.

Bmp4 Made by Extraembryonic Mesoderm Affects PGC Localization and Survival. Unlike the PGCs in control chimeras, most of the PGCs present in $Bmp4^{lacZ/tm1}$ tetraploid chimeras at the pre-somite stage are not localized at the base of allantois but are dispersed throughout the yolk sac, amnion, and allantois. In one case, PGCs may possibly have aggregated into a large clump within the allantois (Table 1). This mislocalization may be the result of defects extrinsic to the PGCs or defects in the PGCs themselves (or both). For example, the mesenchyme cells around the PGCs or the presumptive hindgut endoderm with which they later associate (2, 3) may require Bmp4 to differentiate correctly and to produce the chemoattractants, chemorepellants, or extracellular matrix factors that normally either promote or restrict PGC migration and behavior. Alternatively, Bmp4 in the ExM may directly or indirectly affect the differentiation of the PGCs, and their expression of receptors for extracellular matrix proteins or adhesion molecules, or cellular machinery needed for response to guidance cues in the environment. The abnormal morphology of PGCs in the mutant chimeras supports the idea that these cells are not interacting normally with their environment and may be undergoing a high rate of apoptosis. For whatever reason, if the PGCs are unable to actively move into the hindgut endoderm, they may be passively swept into the yolk sac or allantois, as argued by others (2, 21).

By the early somite stage, the overall number of PGCs in $Bmp4^{lacZ/tm1}$ tetraploid chimeras has declined, relative to earlier stages, to control chimeras. The reduction is seen in both ectopic and normal locations, suggesting that the loss, presumably by apoptosis (Fig. 2 *H* and *I*), is not just due to PGCs being in an abnormal location. The apparent failure of PGCs in the hindgut pocket to survive may be due to defects in the local environment or to the fact that, in the absence of Bmp4, PGCs do not express receptors for survival factors. A number of candidates have been identified as survival factors for early PGCs *in vivo*, including Fgfs, stem cell factor, and members of the IL-6/LIF cytokine family (3). We have shown here that *Fgf8* is still expressed in the posterior of $Bmp4^{lacZ/tm1}$ tetraploid chimeras, but we have not yet investigated the expression of other potential PGC survival factors or the possibility that Bmp4 itself functions as a survival factor in the ExM.

Requirement of Bmp4 for the Growth and Differentiation of the Allantois. In all *Bmp4*$^{lacZ/tm1}$ tetraploid chimeras examined an allantois-like structure is formed that expresses at least one allantois marker. However, the allantois is always abnormal in size and morphology and fails to fuse with the chorion. The absence of *Bmp4* expression in the ExM has no significant effect on the overall proliferation rate of allantois cells. However, at the presomite stage, mutant chimeras have a marked deficiency of both Flk1-positive angioblasts and Pecam1-expressing blood vessels. This deficiency suggests that locally produced Bmp4 protein plays two roles in allantois vasculogenesis, the first in promoting differentiation of allantoic mesoderm cells into angioblasts and/or in the survival of these cells once they have formed, and the second in promoting the assembly of endothelial cells into organized blood vessels. Finally, the absence of VCAM-1 expression may be due to a failure in the initial formation of an outer layer of mesothelium in the absence of *Bmp4* expression in the allantoic mesoderm, or to a defect in the differentiation of any mesothelial cells that are present.

Potential Signaling Components Mediating the Effect of Bmp4 on PGCs and the Allantois. Implicit in the discussion above is that cells of the allantois and ExM, and possibly also the PGCs, express Bmp4 receptors and downstream signaling components such as Smad1, -5, -8, and -4 (reviewed in ref. 22). Genes encoding these proteins have widespread expression at the presomite and early somite stages (23, 24). Recent studies have shown that *Smad1* null mutants have few PGCs and allantois defects, albeit less severe than described here (25). In *Smad5* null mutants the founding population of PGCs is significantly smaller than normal, and they become ectopically localized in the ExM, as described here. The differentiation of the allantois and amnion is also abnormal, suggesting defects in mesodermal lineage allocation and/or cell behavior within the ExM (21). These results are consistent with overlapping functions for both *Smad1* and *Smad5* in the induction of PGC precursors in the epiblast and the differentiation of ExM cells and PGCs once they are formed, but not in the actual allocation of precursors to the germ cell or somatic lineages. The model outlined in Fig. 4 has yet to be completed by identification of the Bmp receptors involved and the downstream target genes of Bmp signaling in each cell population.

We thank Andras Nagy and Marina Gertsenstein for precious and informative advice on making chimeras. We thank Kirstie Lawson for critically reading the manuscript. We also thank Angela D. Land-Dedrick for assistance in manuscript preparation. T.F. was supported by a grant from the National Institutes of Health (HD 28955) to B.L.M.H., who is an Investigator of the Howard Hughes Medical Institute.

1. Lawson, K. A. & Hage, W. J. (1994) *Ciba Found. Symp.* **182,** 68–84.
2. Anderson, R., Copeland, T. K., Scholer, H., Heasman, J. & Wylie, C. (2000) *Mech. Dev.* **91,** 61–68.
3. Tsang, T. E., Khoo, P. L., Jamieson, R. V., Zhou, S. X., Ang, S. L., Behringer, R. & Tam, P. P. L. (2001) *Int. J. Dev. Biol.* **45,** 549–556.
4. Yoshimizu, T., Obinata, M. & Matsui, Y. (2001) *Development (Cambridge, U.K.)* **128,** 481–490.
5. Lawson, K. A., Dunn, N. R., Roelen, B. A., Zeinstra, L. M., Davis, A. M., Wright, C. V., Korving, J. P. & Hogan, B. L. (1999) *Genes Dev.* **13,** 424–436.
6. Ying, Y., Liu, X. M., Marble, A., Lawson, K. A. & Zhao, G.-Q. (2000) *Mol. Endocrinol.* **14,** 1053–1063.
7. Ying, Y. & Zhao, G.-Q. (2001) *Dev. Biol.* **232,** 484–492.
8. Ying, Y., Qi, X. & Zhao, G.-Q. (2001) *Proc. Natl. Acad. Sci. USA* **98,** 7858–7862. (First Published June 26, 2001; 10.1073/pnas.151242798)
9. Nagy, A., Rossant, J., Nagy, R., Abramow-Newerly, W. & Roder, J. C. (1993) *Proc. Natl. Acad. Sci. USA* **90,** 8424–8428.
10. Winnier, G., Blessing, M., Labosky, P. A. & Hogan, B. L. (1995) *Genes Dev.* **9,** 2105–2116.
11. Hogan, B. L. M., Beddington, R., Constantini, F. & Lacy, E. (1994) *Manipulating the Mouse Embryo* (Cold Spring Harbor Lab. Press, Plainview, NY).
12. Crossley, P. H. & Martin, G. R. (1995) *Development (Cambridge, U.K.)* **121,** 439–451.
13. Downs, K. M. & Harmann, C. (1997) *Development (Cambridge, U.K.)* **124,** 2769–2780.
14. Downs, K. M., Gifford, S., Blahnik, M. & Gardner, R. L. (1998) *Development (Cambridge, U.K.)* **125,** 4507–4520.
15. Downs, K. M. & Bertler, C. (2000) *Anat. Embryol.* **202,** 323–331.
16. Gurtner, G. C., Davis, V., Li, H., McCoy, M. J., Sharpe, A. & Cybulsky, M. I. (1995) *Genes Dev.* **9,** 1–14.
17. Kwee, L., Baldwin, H. S., Shen, H. M., Stewart, C. L., Buck, C., Buck, C. A. & Labow, M. A. (1995) *Development (Cambridge, U.K.)* **121,** 489–503.
18. Yang, J. T., Rayburn, H. & Hynes, R. O. (1995) *Development (Cambridge, U.K.)* **121,** 549–560.
19. Downs, K. M., Temkin, R., Gifford, S. & McHugh, J. (2001) *Dev. Biol.* **233,** 347–364.
20. Coucouvanis, E. & Martin, G. R. (1999) *Development (Cambridge, U.K.)* **126,** 535–546.
21. Chang, H. & Matzuk, M. M. (2001) *Mech. Dev.* **104,** 61–67.
22. Massague, J. & Chen, Y. G. (2000) *Genes Dev.* **14,** 627–644.
23. Chang, H., Huylebroeck, D., Verschueren, K., Guo, Q., Matzuk, M. M. & Zwijsen, A. (1999) *Development (Cambridge, U.K.)* **126,** 1631–1642.
24. Mishina, Y., Suzuki, A., Ueno, N. & Behringer, R. R. (1995) *Genes Dev.* **9,** 3027–3037.
25. Tremblay, K. D., Dunn, N. R. & Robertson, E. J. (2001) *Development (Cambridge, U.K.)* **128,** 3609–3621.